

Thermally Stable Multicomponent Manganese Catalyst for the Deep Oxidation of Methane to CO₂

N. M. Popova, K. D. Dosumov, Z. T. Zheksenbaeva, L. V. Komashko,
V. P. Grigor’eva, A. S. Sass, and R. Kh. Salakhova

Sokol’skii Institute of Organic Catalysis and Electrochemistry, Academy of Sciences of Kazakhstan, Almaty, Kazakhstan

e-mail: orgcat@nursat.kz

Received March 22, 2005

Abstract—A thermally stable manganese oxide catalyst for the deep oxidation of lean CH₄ mixtures with air to CO₂ was developed and characterized. To prepare this catalyst, new approaches to the synthesis of polyoxide catalysts based on Mn modified with La, Ce, Ba, and Sr by supporting them from nitrate solutions onto alumina granules stabilized with 2% Ce were used. The catalyst gave the degree of CH₄ oxidation to CO₂ at a level of 90–98% at a CH₄ concentration of 0.2–4.0% in air (space velocity of 10×10^3 h⁻¹; temperature of 973 K). The heating of a Mn-containing sample in air to 1373 K had no negative effect on the conversion of CH₄; an insignificant decrease in the catalyst activity (by ~10%) was observed only on heating above 1473 K. The degree of CH₄ oxidation to CO₂ depended only slightly on O₂ and CH₄ concentrations varied over the ranges 2–20 and 0.5–4.0%, respectively. With the use of physicochemical techniques (XRD analysis, BET, electronic diffuse-reflectance spectroscopy, TPD, TPR, and TPO), it was found that the catalyst underwent considerable phase transformations as the temperature was increased to 1473 K: Mn₂O₃ clusters, which occurred at 873 K, were partially converted into LaMnO₃ perovskites above 1173 K or LaMnAl₁₁O₁₉ hexaaluminates above 1273 K. Oxygen that is the constituent of the latter species participated in the oxidation of CH₄ to CO₂.

DOI: 10.1134/S0023158406060140

INTRODUCTION

The catalytic oxidation of methane from oil and coal deposits without the formation of nitrogen oxides is a promising process for the utilization of natural methane and other alkanes. Heat, carbon dioxide, and products usable in organic synthesis (CO and H₂) can be obtained by this process. As calculated, the cost of heat produced by methane combustion in a pilot plant at a CH₄ concentration of 0.60–0.85% is 15–18 rubles per Gcal [1], which is lower than that in a coal boiler plant.

The catalytic processes of fuel combustion for heat production have found practical use in heaters developed at the Institute of Physical Chemistry of the USSR Academy of Sciences, in various local heating devices in the systems of two-stage fuel combustion (IG, National Academy of Sciences of Ukraine), and in catalytic moving-bed heat generators with the use of the reverse supply of a reaction mixture (Boreskov Institute of Catalysis, Siberian Division, Russian Academy of Sciences, Novosibirsk).

It is well known that Co, Cu, Mn, and Cr oxides and, in some cases, Ni oxides, on which the heat of oxygen adsorption is low, exhibit the highest activity in the reaction of methane oxidation. Among the perovskite-type mixed oxides ABO₃, systems with a minimum energy of the B–O bond exhibit a maximum efficiency. By this is meant that the catalytic activity depends on

the cations of B in an octahedral coordination. Very rigid requirements are imposed on catalysts for the deep oxidation of CH₄ and other hydrocarbons: along with high activity and selectivity, they should exhibit high thermal stability (to 1473 K) and mechanical strength.

An analysis of technical and patent publications indicated that several types of catalysts have found use in CH₄ oxidation processes: supported noble metals (Pt and Pd), spinels, perovskites, manganese oxide catalysts with or without Pd added, and hexaaluminates containing lanthanum and manganese [2, 3]. A cobalt–chromium catalyst on silica fiber as slabs, as well as on metal honeycomb supports, was an early catalyst used in catalytic heaters [4, 5]. In recent years, new heat-conducting reinforced porous 5–5.5% Pt and Pd metal catalysts [6] as flat and corrugated ribbons were developed at the Boreskov Institute of Catalysis, Siberian Division, Russian Academy of Sciences (Novosibirsk). They are used in various heat-generating devices for the combustion of propane–butane mixtures [7].

Attention has been focused on the development of palladium catalysts modified with rare earth elements (REEs) and ZrO₂ and mixed platinum catalysts on various supports. Catalysts that are active in hydrocarbon oxidation processes contain platinum as Pt⁰ and palladium in an oxidized state. Palladium catalysts, in which

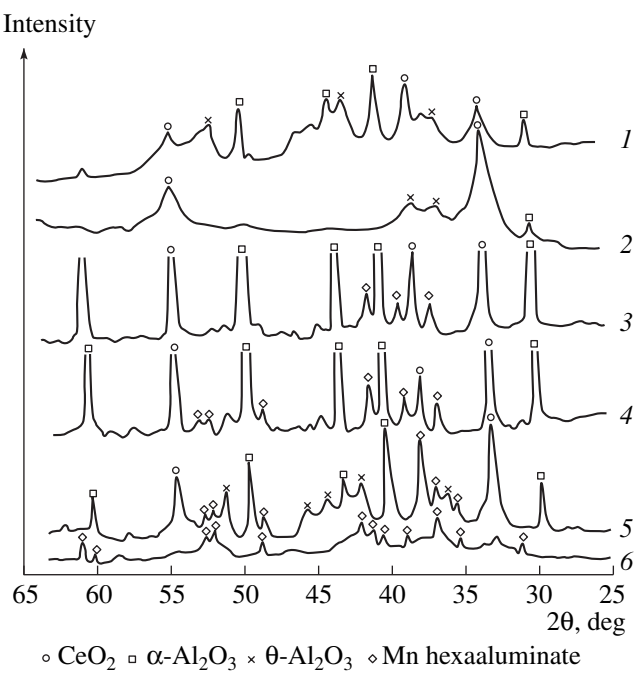


Fig. 1. XRD patterns of samples after drying and heating in air: (1) 2% Ce/(θ-Al₂O₃ + α-Al₂O₃) support (heating at 873 K for 1 h), (2) Ce–Sr–Ba–La–Mn/2% Ce/(θ-Al₂O₃ + α-Al₂O₃) catalyst (873 K, 1 h), (3) Ce–Sr–Ba–La–Mn/2% Ce/(θ-Al₂O₃ + α-Al₂O₃) (1473 K, 20 h), (4) Ce–Sr–Ba–La–Mn/2% Ce/(θ-Al₂O₃ + α-Al₂O₃) + 0.3% Pt (1473 K, 20 h), (5) Ce–Sr–Ba–La–Mn–Al₁₁O₁₉/2% Ce on a (θ-Al₂O₃ + α-Al₂O₃) microsphere (1373 K, 2 h; the sample was synthesized by precipitation with ammonia), and (6) La_{0.8}Ba_{0.2}MnAl₁₁O₁₉ (1373 K, 2 h; unsupported sample synthesized by precipitation with NH₄OH).

Pd⁰ is formed as a result of PdO degradation at high temperatures, frequently undergo deactivation [8–10]. Rare earth, nickel, zirconium, and cobalt oxides, which form mixed oxides with Pd [8, 10–13] to enhance the stability of Pd⁺ and Pd^{δ+} ions to reduction, are used for the stabilization of these catalysts.

Catalysts based on complex oxides (ABO₃ perovskites synthesized by various methods [14–16]), which give materials with nanoperiodic structures [17], were proposed for the combustion of CH₄. It is well known that the transition element B in the structure of ABO₃ occurs in an octahedral coordination, which is favorable for oxidation reactions, and it is characterized by a low activation energy of the M³⁺ → M²⁺ transition (M is a metal). Attention is focused on the preparation of bulk and ceramic-supported perovskites in which the element B is Co, Fe, or Mn [18–21]. It was found that the activity of perovskites in the CH₄ oxidation reaction decreased in the order LaMnO₃ > LaCoO₃ > LaFeO₃. The synthesis of catalysts at a high temperature increases their defectiveness; facilitates the formation of oxygen vacancies; decreases the energy of M–O bonds; and, ultimately, increases the catalyst activity.

Pod'yacheva [20] attempted to support the perovskite LaCoO₃ on high-permeability metal honeycomb materials; however, the activity of the resulting catalysts was tested only at low space velocities (1 × 10³ h⁻¹).

Preparation procedures for catalysts based on manganese oxide were proposed [22–27]. These catalysts are used both in nonstationary combustion processes with heat utilization and for the neutralization of waste gases. Copper oxide and mixed oxide catalysts based on Cu, Ni, and Cr are used for methane oxidation and the removal of trace hydrocarbons from inert gases and oxygen [28–30].

Unfortunately, the majority of well-known oxide and mixed catalysts (other than hexaaluminate) do not withstand the high temperatures at which the combustion of CH₄ in heat generators and gas turbines takes place. Moreover, water vapor and poisons (SO₂) have an adverse effect on these catalysts. At high temperatures, poisons react with a support and undesirable phase transformations occur, which can be partially inhibited by the modification of aluminum oxide with lanthanum and other rare earth oxides.

Among oxide catalysts, a manganese catalyst prepared by the interaction of aluminum hydroxide and manganese nitrate followed by drying and heating at 1223 K [27], as well as a Ni–Cu–Cr catalyst on Ce/θ-Al₂O₃ [28–31], exhibited the highest stability (to 1273 K).

In this work, in order to enhance the thermal stability of a manganese catalyst to 1473 K, we added Group II and Group III elements (Ba, Sr, La, and Ce) as catalyst constituents and used cerium-modified θ-Al₂O₃ as a support. Previously [14], it was found that an optimum ratio between elements in a catalyst for CO oxidation is described by the proportion Ba : Sr : La : Ce : Mn = 1 : 1 : 1 : 7 : 10, which corresponds to the stoichiometry of oxides in the perovskite structure.

EXPERIMENTAL

The catalyst was prepared by the incipient wetness impregnation of a 2% Ce/θ-Al₂O₃ promoted support granules ($d = 4\text{--}5\text{ mm}$; $S_{sp} = 100\text{ m}^2/\text{g}$) with a mixture of aqueous solutions of Mn, Ba, Sr, La, and Ce nitrates followed by drying at 450–470 K and heating at 873 K in air for 1 h. The θ-Al₂O₃ support contained α-Al₂O₃ traces. It was found that mixed complexes of the elements with the surface OH groups of Al₂O₃ were formed on the surface after impregnation; then, the dehydration and decomposition of element nitrates occurred. The elimination of physically adsorbed water occurred at 350–370 K; the dehydration occurred at 440–460 K (an endothermic effect); the decomposition of manganese nitrates occurred at 560–620 K (an exo effect); and the decomposition of rare earth nitrates and alkaline earth nitrates and the formation of oxides occurred at 780–873 K.

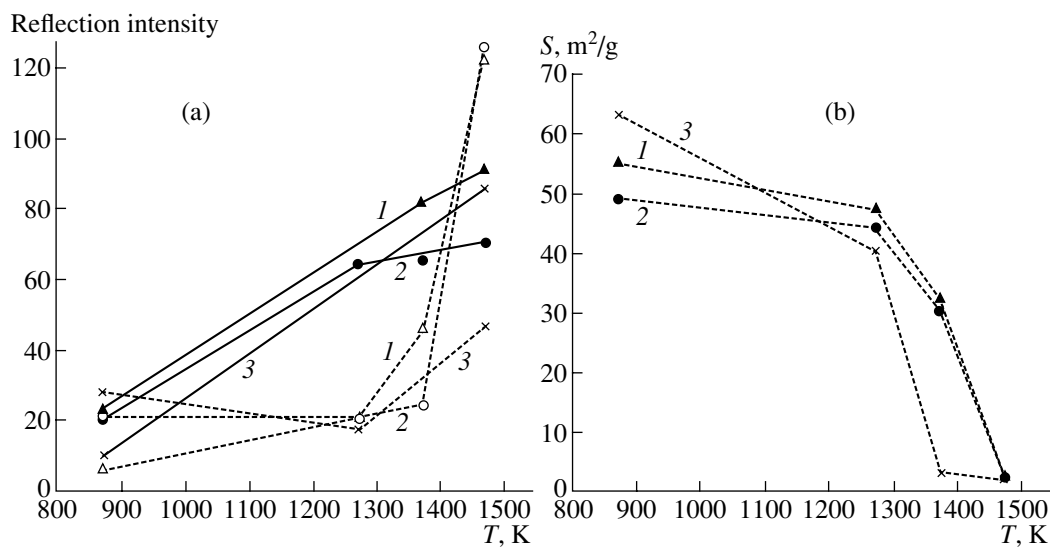


Fig. 2. Effects of heating temperature on (a) the reflection intensities of (solid lines) CeO_2 (1.91 Å) and (dashed lines) $\alpha\text{-Al}_2\text{O}_3$ (1.74 Å) and (b) the total specific surface area in (1) the 7.5% Mn-REE-AEE/2% Ce/0-Al₂O₃ catalyst and the above catalyst with (2) Pt or (3) Pd added after heating in air (for 5 h at each temperature).

To study the effect of promoters, small amounts of Pt (0.3%) and Pd (0.05%) were introduced into the catalyst over the components supported in combination. The activity of catalysts was determined in a flow system by performing a reaction of methane oxidation in a mixture with air (0.5% CH_4) at a space velocity of $10 \times 10^3 \text{ h}^{-1}$ and a temperature of 673–973 K. The analysis for CH_4 and the resulting CO_2 was performed on an LKhM-72 chromatograph with the use of a katharometer. The greatest degree of oxidation at 973 K was reached on a catalyst containing 7.0–7.5 wt % active components (~3 wt % Mn), particularly after catalyst heating at 1473 K. In the study of the effects of process parameters, the space velocity was varied from 10×10^3 to $20 \times 10^3 \text{ h}^{-1}$ and the concentrations of O_2 and CH_4 were varied from 2 to 20 and from 0.2 to 4%, respectively. The thermal stability was tested by heating samples in air at 873 K for 1 h (standard treatment) and then sequentially at 1073, 1273, 1373, and 1473 K for 5 h at each temperature.

X-ray diffraction (XRD) analysis, emission spectroscopic analysis, microdiffraction electron microscopy, the BET method, electronic diffuse-reflectance spectroscopy, temperature-programmed desorption (TPD) of oxygen, temperature-programmed reduction (TPR) of samples with hydrogen, and temperature-programmed oxidation (TPO) of the samples with oxygen were used in order to determine the chemical and phase compositions, morphology, particle sizes, and surface areas of catalysts and the adsorption and reactivity of oxygen.

RESULTS

XRD Analysis and Electron Microdiffraction

The presence of $\theta\text{-Al}_2\text{O}_3$ (35-121 JCPDS) (lines at 2.44, 2.73, 1.39, and 2.84 Å) and an amount of $\alpha\text{-Al}_2\text{O}_3$ (10-173 JCPDS) (lines at 2.09, 2.55, 1.60, and 1.74 Å), as well as crystalline CeO_2 (34-394 JCPDS) (lines at 3.12, 2.16, 2.54, and 2.49 Å), was detected by XRD (Fig. 1) in the initial 7.5% Mn catalyst (Mn-REE-AEE/2% Ce/0-Al₂O₃), where AEE refers to an alkaline earth element) after heating at 873 K in air [32].

According to XPS data, cerium occurred in the catalyst in the oxidation state Ce^{4+} ($E_b = 891.1 \text{ eV}$). After heating at 1170 K for 20 h, the electron binding energy is $E_{3d_{5/2}} = 887.0 \text{ eV}$ (which corresponds to Ce^{3+}).

Long-term heating with a gradual increase in the temperature affected the total surface area and phase composition of the 7.5% Mn-REE-AEE catalyst. The $\alpha\text{-Al}_2\text{O}_3$ and CeO_2 concentrations were quantitatively evaluated from the intensities of reflections at 1.74 and 1.91 Å in the XRD pattern. It can be seen in Fig. 2 that the concentration of crystalline CeO_2 in the catalyst increased as the catalyst was heated, whereas the formation of $\alpha\text{-Al}_2\text{O}_3$ was dramatically enhanced above 1273 K. This was accompanied by an insignificant decrease in the specific surface area at temperatures to 1273 K and a dramatic decrease to 2–5 m^2/g at 1473 K.

Platinum and palladium promotion had an insignificant effect on the phase composition and specific surface area of catalysts. Lines that corresponded to the crystals of Ba, Sr, La, and Mn oxides were not detected in the X-ray diffraction patterns of catalysts heated at 1273–1473 K; this fact is indicative of the high extent of dispersion of these crystals and of their stability to

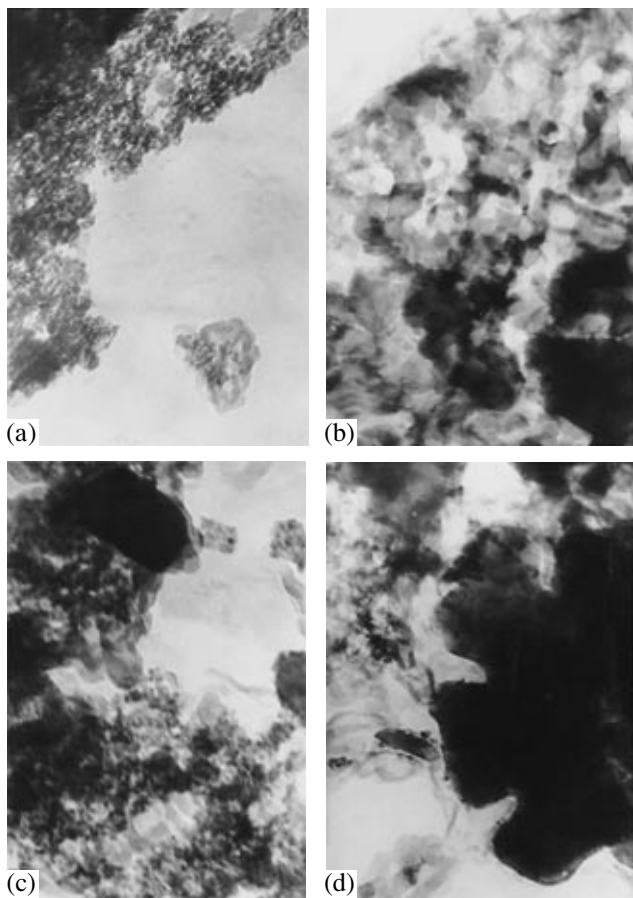


Fig. 3. Electron micrographs (magnification of 1.6×10^5) of the 7.5% Mn-REE-AEE/2% Ce/θ-Al₂O₃ catalyst (a) after heating at 873 K, (b) after promoting with Pt and heating at 873 K, (c) after promoting with Pd and heating at 873 K, and (d) after heating the foregoing sample at 1273–1473 K.

agglomeration. At heating temperatures of 1273 K or higher, reflections were detected at 2.64, 2.50, and 2.80 Å, which were assigned to manganese hexaaluminates. As the heating temperature was increased from 1273 to 1473 K, the line intensity at 2.80 Å increased

from 10 to 20, from 13 to 23, or from 7 to 10 arbitrary units for the Mn-REE-AEE catalyst, the sample with a Pd additive, or the sample with a Pt additive, respectively.

In the X-ray diffraction pattern of the Mn-REE-AEE catalyst, which was prepared by the precipitation of elements on a Ce/θ-Al₂O₃ microsphere with ammonia, the number and intensity of lines corresponding to the hexaaluminate LaMnAl₁₁O₁₉ increased [3] and the resulting pattern was practically identical to that corresponding to La_{0.8}Ba_{0.2}MnAl₁₁O₁₉ (Fig. 1, curves 5, 6).

An analysis of electron micrographs (Fig. 3a) and microdiffraction data (see table) indicated that small particles of Mn (Mn₂O₃), Ba, Sr, and Ce oxides ($d = 30$ –40 Å) and translucent dense particles of various aluminates (LaAlO₃, CeAlO₃, and LaMnAl₁₁O₁₉) with signs of faceting ($d = 70$ –100 Å) [33] were present in the initial 7.5% Mn-REE-AEE catalyst supported on 2% Ce/θ-Al₂O₃ (heating temperature of 873 K). The sample promoted with Pt (Fig. 3b) exhibited small particles ($d = 50$ –100 Å) of the clusters of Ba, Ce, La, Pt, and Sr oxides and Mn₂AlO₄ and translucent clustered platelike prismatic crystals ($d = 200$ Å and above), as well as the flakes of a mixture of Mn₂AlO₄, LaPt, Mn₃O₄, LaMnAl₁₁O₁₉, SrAl₁₂O₁₉, and BaMnO₄.

The sample promoted with Pd (Fig. 3c) also exhibited small oxide particles (100–200 Å); medium and coarse translucent Mn₂AlO₄ and CeAlO₃ aluminate particles; and coarse translucent Sr₃Al₃₂O₅₁, LaMnAl₁₁O₁₉, and SrMnO₃ formations. The heating of Mn catalysts promoted with platinum and palladium at 1373–1473 K resulted in a considerable coarsening of both oxide and aluminate particles. The aluminates of Sr, Mn, and Ce and the mixed oxides Ba(MnO₄)₂ appeared (Fig. 3d).

Thus, with the use of electron microscopy and microdiffraction, we found that all of the supported components partially reacted with θ-Al₂O₃, although it was protected with cerium (CeAlO₃), even at 873 K along with the formation of small oxide cluster particles in the initial Mn-REE-AEE/Ce/θ-Al₂O₃ catalyst. Heating at a high temperature (1273–1473 K), especially in the presence of Pt and Pd, resulted in the for-

Electron-microscopic study of 7.5% Mn-REE-AEE polyoxide catalysts on 2% Ce/θ-Al₂O₃

Catalyst	Heating temperature, K	Particle size, Å	Composition
Ba–Sr–La–Ce–Mn	873	30–40	Mn ₂ O ₃ and Ba, Sr, and Ce oxides
		70–100	LaMnAl ₁₁ O ₁₉ , LaAlO ₃ , CeAlO ₃
Ba–Sr–La–Ce–Mn + Pd	873	100–200	Mn ₂ AlO ₄ , CeAlO ₃ , Sr ₃ Al ₃₂ O ₅₁ , LaMnAl ₁₁ O ₁₉ , SrMnO ₃
		>200	Sr, Mn, and Ce aluminates and Ba(MnO ₄) ₂ mixed oxides
Ba–Sr–La–Ce–Mn + Pt	873	50–100	Ba, Ce, La, Pt, and Sr oxides and Mn ₂ AlO ₄
		100–200	LaMnAl ₁₁ O ₁₉ , Mn ₂ AlO ₄ , LaPt, SrAl ₁₂ O ₁₉ , BaMnO ₄ , Mn ₃ O ₄
	1473	>200	Mn ₂ AlO ₄ , CeAlO ₃ , LaMnAl ₁₁ O ₁₉ , and Ba(MnO ₄) ₂ mixed oxides

mation of mixed oxides from dispersed Ba, Sr, La, and Mn oxides, and the entire support surface was coated with a continuous crust of the reaction products of supported components and $\theta\text{-Al}_2\text{O}_3$; structurally different aluminates, primarily, $\text{LaMnAl}_{11}\text{O}_{19}$ in a hexagonal syngony.

Electronic Diffuse-Reflectance Spectra

To obtain the diffuse-reflectance spectra of catalysts, a Shimadzu UV-300 instrument equipped with a standard attachment for reflectance measurements in the region 240–800 nm was used. The measurements were performed in air. Aluminum oxide calcined at an appropriate temperature served as a reference sample [34].

Figure 4 shows the electronic diffuse-reflectance spectra of a Mn catalyst supported on $\chi\text{-Al}_2\text{O}_3$ and catalysts with alkaline earth oxide and rare earth oxide additives, as well as a mixture of alkaline earth oxides and rare earth oxides. The samples were heated at 873 and 1173 K.

Strong absorption in the visible region at λ of above 400 nm and a maximum at $\lambda = 340\text{--}350$ nm are characteristic of $\text{Mn}/\text{Al}_2\text{O}_3$ heated at 873 K (Fig. 4, spectrum 1). An absorption band at 340–350 nm corresponds to the $\text{Mn}^{3+} + \text{O}^{2-} \rightarrow \text{Mn}^{2+} + \text{O}^-$ charge transfer in oxide clusters [35]. It indicates the formation of a dispersed Mn_2O_3 oxide phase, which was not detected in the XRD pattern [34]. After heating at 1173 K, an increase in absorption in the region 240–320 nm was observed and the position of a maximum shifted to 320 nm (spectrum 2). Moreover, the absorption increased in the region of 360–420 nm and decreased above 550 nm. In the visible region of the spectrum, an absorption maximum was observed at 440–460 nm and its position coincided with the position of the $\text{Mn}_{\text{octa}}^{3+}$ charge-transfer band. According to Vorob'ev et al. [35], the appearance of an absorption band in the region 400–530 nm suggests the formation of Mn^{4+} . It is likely that a maximum at 320 nm resulted from the superposition of absorption bands due to Mn^{4+} (below 300 nm) and Mn^{3+} (a maximum at $\lambda = 340$ nm).

The addition of barium and strontium oxides had almost no effect on the shape of the spectrum of an initial $\text{Mn}/\text{Al}_2\text{O}_3$ sample, whereas the addition of a rare earth oxide decreased the intensity of absorption in the visible region of the spectrum at $\lambda > 550$ nm (spectrum 4). The observed difference suggests a decrease in the concentration of a manganese oxide phase upon the introduction of cerium and lanthanum. An increase in the heating temperature of an $\text{Mn AEE}/\text{Al}_2\text{O}_3$ sample to 1173 K caused a decrease in absorption in the region of 240–320 nm. An absorption maximum at 320–340 nm in the UV region indicates that, unlike the $\text{Mn}/\text{Al}_2\text{O}_3$ sample (spectrum 2), the formation of Mn^{4+} ions is hindered in this case, probably because of the stabilization of an

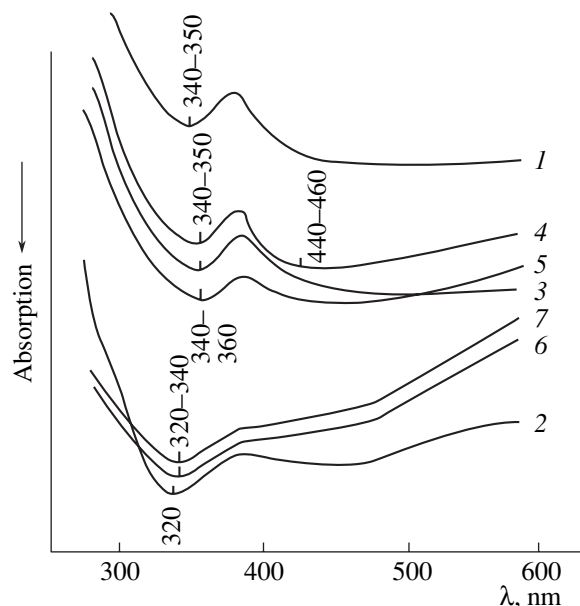


Fig. 4. Electronic diffuse-reflectance spectra of Mn catalysts supported on $\chi\text{-Al}_2\text{O}_3$ (1, 2) without additives and with (3) alkaline earth oxide, (4, 7) rare earth oxide, and (5, 6) mixed rare earth and alkaline earth oxide additives: heating temperature of (1, 3–5) 873 or (2, 6, 7) 1173 K.

Mn_2O_3 phase on Al_2O_3 . After the treatment of an $\text{Mn REE}/\text{Al}_2\text{O}_3$ sample at 1173 K, a further decrease in the intensity of absorption in the region above 500 nm was observed, which corresponds to a considerable decrease in the concentration of the Mn_2O_3 oxide phase. Characteristic changes that indicate the formation of Mn^{4+} ions were absent from the spectrum. The spectrum of a manganese catalyst with rare earth and alkaline earth oxides heated at 1173 K (spectrum 6) was practically identical to the spectra of $\text{Mn-REE}/\text{Al}_2\text{O}_3$ (spectrum 7). From this it follows that rare earth elements have a crucial effect on the state of manganese supported on Al_2O_3 ; because of the stabilization of rare earth metal ions in the support structure, they prevent the formation of Mn^{4+} ions. Simultaneously, the concentration of a dispersed phase of Mn_2O_3 decreased. The absence of an absorption maximum at 320 nm, which is indicative of the above fact, and absorption bands in the region of 400–500 nm (Mn^{4+}) can be a consequence of the dispersion of the Mn_2O_3 phase to ions and the interaction of these ions with rare earth oxides from perovskite. The possibility of perovskite–kurnakovite formation based on manganese and rare earth oxides at the specified temperatures was noted by Rode in his monograph [36].

Thermal Desorption of Oxygen

Previously, we studied the thermal desorption of oxygen from 7% $\text{Mn-REE-AEE}/(\gamma\text{-Al}_2\text{O}_3 + \theta\text{-Al}_2\text{O}_3)$ and $\text{Mn}/(\gamma\text{-Al}_2\text{O}_3 + \theta\text{-Al}_2\text{O}_3)$ catalysts [37]. In TPD from the $\text{Mn}/\text{Al}_2\text{O}_3$ sample, three peaks were observed,

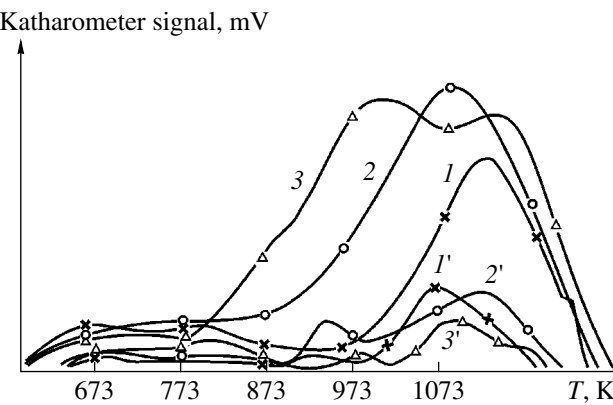


Fig. 5. Spectra of the TPD of oxygen from (1, 1') the Mn-REE-AEE/2% Ce/θ-Al₂O₃ catalyst and samples promoted with (2, 2') Pd or (3, 3') Pt. Heating temperature: (1–3) 873 or (1'–3') 1473 K.

which corresponded to the desorption of (a) adsorbed oxygen (473–773 K), (b) oxygen from the MnO₂ oxide, which decomposed with the formation of β-Mn₂O₃ (723–923 K), and then (c) Mn₃O₄ and MnO (923–1173 K). The activation energies of desorption (E_{des}) for these three compounds were 77.9–80.2, 94.3–98.6, and 115–142.1 kJ/mol, respectively. On the addition of Group II and Group III elements, the formation of MnO₂ considerably decreased, the amount of weakly bound adsorbed oxygen increased, and the release of oxygen increased in the region where the degradation of Mn₂O₃ occurred, whereas the corresponding peak shifted toward lower temperatures. The amount of oxygen released in the Mn₂O₃ degradation region was higher than a stoichiometric amount; this fact was explained by the partial formation of new polyoxide compounds like AMnO₃ containing superstoichiometric oxygen.

In the thermal desorption spectrum of the Mn-REE-AEE/2% Ce/θ-Al₂O₃ catalyst after heating at 873 K and O₂ adsorption at 673 K, the amounts of adsorbed oxygen and oxygen released in the temperature region of the decomposition Mn₂O₃ → Mn₃O₄ →

MnO considerably decreased (Fig. 5). The major portion of oxygen was released above 1000 K. The promotion of the catalyst with platinum and palladium facilitated an increase in the desorption of oxygen above 773 K.

The heating of the Mn-REE-AEE/2% Ce/θ-Al₂O₃ sample at 1473 K for 5 h caused a significant decrease in the amounts of adsorbed oxygen and oxygen released from the catalyst structure above 973 K and a decrease in E_{des} by 10–20 kJ/mol. As found by emission spectroscopic analysis, these results are related to interactions with the support on heating rather than the escape of manganese and other elements from the catalyst. The thermal desorption spectrum of oxygen from the Mn-REE-AEE/2% Ce/θ-Al₂O₃ samples heat-treated at 1473 K is consistent in shape with the spectrum of oxygen TPD from the hexaaluminate Sr_{1-x}La_xMnAl₁₁O_{19- α} [38].

The results obtained in the study of the thermal desorption of oxygen from Mn-REE-AEE/2% Ce/θ-Al₂O₃ samples heated at 1473 K are fully consistent with XRD and electron microdiffraction data. These results indicate that the release of oxygen on heating was mainly due to the degradation of manganese hexaaluminates and other compounds like BaSrAl₂O₄, LaAlO₃, and SrAl₁₂O₁₉ rather than Mn₂O₃ [33]. In this case, as found in a study of bulk manganese perovskites and hexaaluminates, the concentration of oxygen vacancies in these compounds increased.

Temperature-Programmed Reduction with Hydrogen

The use of TPR allowed us to determine the reactivity of oxygen sorbed by catalysts toward reducing gases. As we found previously, the adsorbed and structural oxygen of the Mn-REE-AEE catalyst supported on γ-Al₂O₃ actively interacts with H₂ at temperatures from 473 to 773 K [37]. An insignificant absorption of H₂ occurred in the region of 875–1173 K; it was due to the reduction of CeO₂. The heating of the catalyst at 1173 K affected only slightly the amount and temperature regions of H₂ absorption.

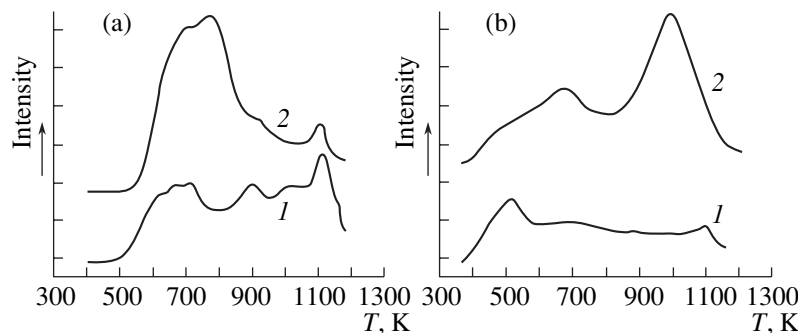


Fig. 6. (a) TPR spectra of (1) Mn-REE-AEE/2% Ce/θ-Al₂O₃ and (2) La_{0.8}Ba_{0.2}MnAl₁₁O₁₉ samples after heating at 1373 K in air and (b) spectra of the temperature-programmed adsorption of O₂ after sample reduction at temperatures to 1173 K.

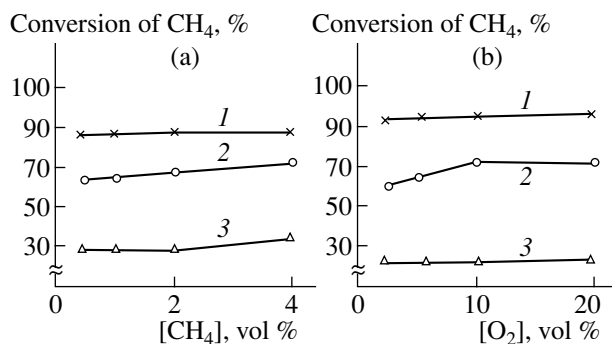


Fig. 7. Effects of (a) CH_4 concentration at $[\text{O}_2] = 10\%$ and (b) O_2 concentration at $[\text{CH}_4] = 0.5\%$ on the degree of CH_4 conversion into CO_2 on the 7.5% Mn-REE-AEE/2% Ce/θ-Al₂O₃ catalyst. Reaction temperatures: (1) 973, (2) 923, and (3) 873 K. $V = 10 \times 10^3 \text{ h}^{-1}$.

Figure 6a shows the TPR spectra of the 7% Mn-REE-AEE/2% Ce/θ-Al₂O₃ and synthesized La_{0.8}Ba_{0.2}MnAl₁₁O₁₉ samples after heating at 1373 K in air. In addition to the absorption of H_2 at 473–873 K (which is also characteristic of a catalyst on γ -Al₂O₃), the absorption of H_2 at temperatures higher than 873 K (a maximum temperature of 873–1173 K) was also observed. Analogous TPR spectra were obtained by Artizzu-Duart et al. [39, 40] in a study of a Ba-Mn hexaaluminate.

The experimental data allowed us to conclude that, in a high-temperature region, hydrogen reacted with oxygen (a constituent of manganese hexaaluminates), which was detected in the course of thermal desorption (see Fig. 5). In this case, the $\text{Mn}^{3+} \rightarrow \text{Mn}^{2+}$ reduction occurred and, simultaneously, oxygen vacancies were formed. In the presence of H_2 , the temperature at which the major portion of structural oxygen was eliminated significantly decreased.

The adsorption of oxygen after the high-temperature heating of reduced samples in an atmosphere of He or $\text{H}_2 + \text{He}$ (Fig. 6b) readily occurred in the regions 373–773 and above 873 K.

Catalytic Activity

In the commercial use of the deep oxidation of CH_4 to CO_2 (heat generation, CH_4 removal from gas vents in coal mines, the production of atmospheres for the storage of agricultural products, and the use of CO_2 for plant nourishment), process conditions (space velocity, reactant concentrations, and catalyst heating temperature), which affect the conversion of CH_4 into CO_2 and various temperatures, are of great importance.

The effects of temperature and space velocity on the conversion of CH_4 (in a concentration of 0.5%) were studied previously [41]. A maximum degree of CH_4 conversion into CO_2 (95–98%) in an air mixture on a 7.0–7.5% Mn-REE-AEE/γ-Al₂O₃ catalyst at 923–

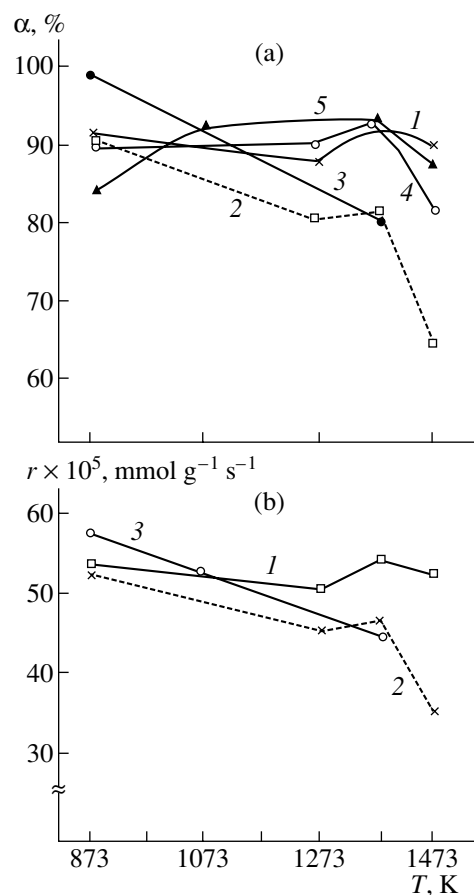


Fig. 8. Effects of catalyst heating temperature on (a) the degree of conversion of 0.5% CH_4 and (b) the specific rate of reaction at $V = 10 \times 10^3 \text{ h}^{-1}$ and 973 K: (1) Mn-REE-AEE/2% Ce/θ-Al₂O₃, (2) Ni-Cu-Cr/2% Ce/θ-Al₂O₃, (3) Mn/Al₂O₃ (IK-40), (4) Mn-REE-AEE with Pd added, and (5) Mn-REE-AEE with Pt added.

973 K was reached at the space velocity $V = (10–15) \times 10^3 \text{ h}^{-1}$.

Figure 7 shows the effect of CH_4 and O_2 concentrations on the degree of CH_4 conversion into CO_2 on 7% Mn-REE-AEE/2% Ce/θ-Al₂O₃ at $V = 10 \times 10^3 \text{ h}^{-1}$. At 973 K and CH_4 and oxygen concentrations from 0.5 to 4 and from 2 to 20%, respectively, the conversion of methane was 90%. At lower temperatures (923 K), the concentration of oxygen in the mixture should be maintained at a level of $\geq 10\%$. The apparent conversions of CH_4 were close to those reached on the LaMnO₃/La/γ-Al₂O₃ catalyst [42].

Figure 8 shows the effects of heating temperature on the degree of conversion (α) and the rate of oxidation (r) of 0.5% CH_4 in air to CO_2 at 973 K on the Mn-REE-AEE/2% Ce/θ-Al₂O₃ catalyst and the samples promoted with Pt and Pd, as well as on the well-known Ni-Cu-Cr oxide catalysts for the deep oxidation of hydrocarbons [28] and on Mn/Al₂O₃ (IK-40) [27]. The degree of methane conversion at 973 K in air on the

Mn–REE–AEE catalyst heated to 1473 K was 88–90%, whereas the rate of oxidation was $(52\text{--}54) \times 10^{-5}$ mmol g⁻¹ s⁻¹. After the heating of the samples promoted with Pt or Pd at 1473 K, the degree of conversion decreased to 81–86%. A more significant decrease in α (to 63%) and r was observed on the Ni–Cu–Cr catalyst. On the IR-40 catalyst, α decreased from 99 to 80% even after heating at 1273 K. A decrease in the catalyst activity at this temperature followed by a more significant decrease at 1473 K was also noted previously [27].

The experimental data are indicative of a higher thermal stability of the Mn–REE–AEE/2% Ce/θ-Al₂O₃ catalyst in the reaction of CH₄ oxidation than that of the well-known oxide catalysts for hydrocarbon oxidation.

DISCUSSION

The study of CH₄ oxidation to CO₂ on Mn catalysts with Ce, La, Ba, and Sr additives supported on 2% Ce/θ-Al₂O₃ under varied process parameters and conditions of the thermal treatment of the samples allowed us to conclude that these catalysts are suitable for the combustion of methane in low concentrations (0.5–4.0%) in air at $V = 10 \times 10^3$ h⁻¹ and 973 K. The catalyst withstood possible overheating to 1473 K.

Let us consider the reasons for the thermal stability of the catalyst under significant changes in its surface and phase composition.

After the decomposition of nitrates in the course of catalyst synthesis and heating in air at 873 K, the presence of CeO₂ crystals, X-ray amorphous Mn₂O₃ clusters ($d = 20\text{--}40$ Å), other oxides, and various dense aluminate and hexaaluminate particles with signs of faceting (70–100 Å) were detected on the support surface using XRD analysis with microdiffraction, electron microscopy, and electronic diffuse-reflectance spectroscopy. Undoubtedly, the active component of this catalyst is the most dispersed Mn₂O₃ oxide, in which manganese occurs in an octahedral coordination and which is characterized by the Mn³⁺ + O²⁻ → Mn²⁺ + O⁻ charge transfer according to electronic diffuse-reflectance spectroscopic data (absorption band at 340–350 nm).

The results obtained by electronic diffuse-reflectance spectroscopy indicate that an increase in the heating temperature to 1173 K facilitated the dispersion of Mn₂O₃. However, on the other hand, it also facilitated the partial interaction of Mn₂O₃ with rare earth oxides to form manganese perovskites. This conclusion was also supported by the study of the TPD of oxygen. At heating temperatures of 873–1173 K, another positive effect of the addition of rare earth and alkaline earth elements, which interact with θ-Al₂O₃ to form CeAl₂O₃, LaAl₂O₃, and other aluminates and prevent manganese from considerable insertion into the support at this stage, manifested itself. Because of this, a relatively high specific surface area (48–55 m²/kg) of the catalyst was retained at heating temperatures to 1273 K.

The catalyst consisted of an X-ray amorphous disperse Mn₂O₃ oxide, which partially formed a solid solution like perovskite (LaMnO₃, BaMnO₄, or SrMnO₄) with rare earth and alkaline earth elements, and CeO₂ crystals. In addition to Mn₂O₃, the resulting perovskites participated in the oxidation reaction.

A further increase in the heating temperature to 1373 K, particularly upon the introduction of promoters (Pt and Pd) as catalyst constituents, resulted in the predominance of CeAlO₃ and Mn₂AlO₄ aluminates and translucent hexagonal formations (Sr₃Al₃₂O₅₁, LaMnAl₁₁O₁₉), which significantly enlarged at 1373–1473 K.

The concentration of the resulting LaMnAl₁₁O₁₉ dramatically increased after heating the sample above 1273 K and upon catalyst promotion with platinum and palladium. Although the θ-Al₂O₃ support was protected with cerium (CeAl₂O₃), manganese interacted with other elements on deep heating. In this case, α-Al₂O₃, Ba–Mn oxides, and manganese aluminates and hexaaluminates ($d = 200$ Å) were formed to result in a considerable decrease in the specific surface area of the catalyst (to 2–4 m²/g). According to published data [2, 3, 38, 39, 43], La–Mn hexaaluminates, as well as the Mn₂O₃ oxide and mixed oxides (manganese perovskites containing Group II and Group III elements), are active and thermally stable catalysts for the deep oxidation of CH₄ to CO₂. It is likely that the formation of La–Mn hexaaluminates is primarily responsible for the retention of the activity of the parent catalyst upon deep heating.

Let us consider how a change in the composition of the Mn–REE–AEE/2% Ce/θ-Al₂O₃ catalyst on heating affects the nature of sorbed oxygen and its participation in the deep oxidation of CH₄.

According to TPD data, adsorbed O₂⁻ and O⁻ (desorption temperature of 613–773 K) and lattice O²⁻ (above 773 K) in Mn₂O₃ and the solid solutions of Mn–rare earth–alkaline earth oxides on 2% Ce/θ-Al₂O₃ are characterized by low activation energies of desorption (80.2, 98.6, and 102.0 kJ/mol, respectively). According to calculation data, the heating of mixed manganese catalysts at 1173 K decreased the activation energies of Mn–O bond rupture and oxygen desorption by 10–20 kJ/mol. In this case, as found in a study of bulk LaMnO₃ perovskites, the concentration of oxygen vacancies in them increased; this facilitated an increase in the activity of the catalyst in the reaction of CH₄ oxidation [19].

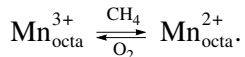
An increase in the heating temperature of the Mn–REE–AEE/2% Ce/θ-Al₂O₃ catalyst from 873 to 1273 K affected only slightly its specific activity:

Heating temperature, K	873	1273	1373	1473
Activity × 10 ⁶ , mmol g ⁻¹ s ⁻¹ m ⁻²	9.4	10.0	17.3	120.0

The point is that activity primarily depends on the concentrations of surface oxygen species (O_2^- , O^-) and lattice oxygen, which is similar to them in terms of E_{des} , in Mn_2O_3 and partially formed perovskites (80–102 kJ/mol). The increase in the specific activity by an order of magnitude upon heating the sample above 1373 K is indicative of the participation of oxygen released from the structures at $T > 973$ K ($E_{des} = 110$ kJ/mol) rather than the surface oxygen of Mn_2O_3 and perovskites, whose concentration dramatically decreased. The participation of this oxygen, which was released at temperatures higher than 928 K, in the oxidation of CH_4 on manganese hexaaluminates was noted previously [3, 39].

According to TPO data (Fig. 6b), oxygen readily entered the structure of the resulting manganese hexaaluminates once again upon heating the sample in an atmosphere of H_2 –He or He at low temperatures because of an increase in the number of oxygen vacancies.

Thus, after the conversion of Mn_2O_3 and manganese perovskites into manganese hexaaluminate compounds at temperatures higher than 1373 K, the structural oxygen of the latter participated in CH_4 oxidation at 973 K. This became possible because of the readily occurring redox reactions



The high activity of manganese hexaaluminates, particularly in the presence of La, Ba, and Sr constituents, which accelerate the synthesis of hexaaluminates at 1470–1570 K, in the oxidation of CH_4 was noted in a number of publications. Under optimum synthesis conditions, the particle diameter of manganese hexaaluminates varied from 200 to 250 nm, and the thickness was 20–40 nm. The $Sr_{0.8}La_{0.2}MnAl_{11}O_{19}$ and $LaMnAl_{11}O_{19}$ hexaaluminates were the most active and stable species [2, 38].

The developed Mn–REE–AEE catalyst on 2% $Ce/\theta-Al_2O_3$ afforded 90–98% conversion of CH_4 into CO_2 at 973 K and $V = 10 \times 10^3$ h⁻¹ and exhibited a higher thermal stability than the well-known oxide catalysts for the deep oxidation of hydrocarbons (Fig. 8).

A similar catalyst supported on $\alpha-Al_2O_3$ blocks was used for the oxidation of CH_4 and a propane–butane mixture in a catalytic heat generator designed for the heating of greenhouses. As found by the analysis of gases formed in the oxidation of hydrocarbons, CO_2 and trace hydrocarbons were present in these gases, whereas nitrogen oxides were completely absent. This fact provides an opportunity to use the resulting CO_2 for plant nourishment in the daytime, which accelerates plant growth and increases the crop capacity.

Thus, the main conclusion drawn from the above study is that a mixed Mn–REE–AEE oxide catalyst on a 2% $Ce/\theta-Al_2O_3$ support exhibits higher thermal stability

(to 1473 K) and specific activity in the deep oxidation of methane, as compared with the well-known IK-40 and $Ni-Cu-Cr/2\% Ce/\theta-Al_2O_3$ catalysts, which are used for the removal of organic substances from gases and the combustion of CH_4 . Its high thermal stability is due to the fact that, unlike $Ni-Cu-Cr/2\% Ce/\theta-Al_2O_3$ and $Mn/\theta-Al_2O_3$ catalysts (in which metal oxides are converted into less active Mn_2AlO_4 , $CuAl_2O_4$, and $NiAl_2O_4$ aluminates on heating in air), the oxide clusters of Mn_2O_3 in the catalyst are dispersed and partially converted into $La(Ce)MnO_3$ perovskites, which contain superstoichiometric oxygen, on heating to 1173 K. The degree of the deep oxidation of methane on the resulting compounds was ~90% at 973 K, and the specific activity of these compounds was close to the activity of Mn_2O_3 (about 10.0×10^{-6} mmol g⁻¹ s⁻¹ m⁻²).

In the case of catalyst overheating to 1473 K, more significant changes in its phase composition occurred due to the formation of $LaMnAl_{11}O_{19}$ hexaaluminates; however, the conversion of CH_4 remained at the same level. In this case, the specific rate of reaction dramatically increased by approximately one order of magnitude and the structural oxygen of hexaaluminates participated in this reaction, whereas the amount of surface oxygen considerably decreased.

The explanation given for the increase in the thermal stability and activity of the Mn–REE–AEE/2% $Ce/\theta-Al_2O_3$ catalyst after long heating at a high temperature is supported by available published data on the properties of manganese hexaaluminates containing Group II and Group III elements [2, 3, 39, 42].

ACKNOWLEDGMENTS

This study was supported by the International Science and Technology Center (grant no. K-270).

REFERENCES

1. Gogin, L.L., *Extended Abstract of Cand. Sci. Dissertation*, Novosibirsk: Inst. of Catalysis, 1996.
2. Machida, M., Sato, A., and Kijima, T., *Catal. Today*, 1995, vol. 26, p. 239.
3. Machida, M., Eguchi, K., and Arai, H., *J. Catal.*, 1990, vol. 123, p. 477.
4. Kadenatsky, B.I., Korobskii, B.S., and Sakeev, A.S., in *Problemy kinetiki i kataliza: glubokoe kataliticheskoe okislenie uglevodorodov* (Problems of Kinetics and Catalysis: Deep Catalytic Oxidation of Hydrocarbons), Moscow: Nauka, 1981, vol. 18, p. 118.
5. Voichenko, A.N., Volchek, Ya.L., Kotyrlo, G.K., and Lezhenin, F.F., *Prom. Teplotekh.*, 1988, vol. 10, no. 6, p. 97.
6. RF Patent 2062402.
7. Luk'yanov, B.N., Kuzin, N.A., and Kirillov, V.A., *Khim. Interes. Ust. Razv.*, 2001, vol. 9, no. 5, p. 667.
8. Farrauto, R.J., Zampert, S.K., and Melvin, C.H., *Appl. Catal., B*, 1995, vol. 6, p. 263.
9. US Patent 4 893 465.

10. Imomoto, K.M., *Shokubai*, 1997, vol. 39, no. 2, p. 62.
11. Wang, J., Sun, Z., and Chen, S., *9th Int. Symp. on Relation between Homo- and Heterogeneous Catalysts*, Southampton, 1998, p. 115.
12. Ivanov, A.V. and Kustov, L.M., *Izv. Akad. Nauk, Ser. Khim.*, 1998, no. 1, p. 57.
13. Popova, N.M. and Savel'eva, G.A., *Teor. Eksp. Khim.*, 1991, no. 6, p. 646.
14. Kosmambetova, G.R., *Extended Abstract of Cand. Sci. Dissertation*, Baku: Inst. of Petrochemical Processes, 1989.
15. Popova, N.M., Kosmambetova, G.R., and Sokolova, L.A., *Second Russian-Korean Joint Seminar on Energy Catalysts*, Novosibirsk, 1997, p. 63.
16. Sokolova, L.A., Kosmambetova, G.R., and Popova, N.M., *Tr. Inst. Org. Katal. Elektrokhim. Akad. Nauk Kaz. SSR*, 1989, vol. 28, p. 199.
17. Bukhtiyarov, V.I. and Slin'ko, M.G., *Usp. Khim.*, 2001, vol. 70, no. 2, p. 167.
18. Mazo, G.N., Kudryashov, I.A., and Kelenitu, N., *Zh. Fiz. Khim.*, 2001, vol. 75, no. 7, p. 1232 [Russ. J. Phys. Chem. (Engl. Transl.), vol. 75, no. 7, p. 1113].
19. Parkhomenko, V.D., Katahinskii, A.S., and Sedyuk, G.N., *Ekotekhnol. Resursosberezh.*, 2000, no. 6, p. 6.
20. Pod'yacheva, O.Yu., *Extended Abstract of Cand. Sci. Dissertation*, Tomsk: Inst. of Petrochemistry, 1998.
21. Cerri, J., Saraeco, Y., and Specchia, V., *Catal. Today*, 2000, vol. 60, p. 21.
22. Matros, Yu.Sh., Gogin, L.L., Lakhmostov, V.S., et al., in *Nestasionarnye protsessy v katalize: tezisy 3 Vses. konf.* (Proc. 3rd All-Union Conf. on Unsteady-State Processes in Catalysis), Novosibirsk, 1986, vol. 1, p. 120.
23. Tsryul'nikov, P.G., Sal'nikov, V.S., Drozdov, V.A., Stukin, S.A., Bubnov, A.V., Grigorov, E.I., Kalinin, A.V., and Zaikovskii, V.I., *Kinet. Katal.*, 1991, vol. 32, no. 2, p. 439.
24. German Patent 20104449.
25. Japanese Patent 52-38977.
26. RF Patent 2063803.
27. RF Patent 1833559.
28. Altynbekova, K.A., *Extended Abstract of Cand. Sci. Dissertation*, Alma-Ata: Inst. of Organic Catalysis and Electrochemistry, 1994.
29. Efrimov, V.N., Golosman, E.Z., Fainshtein, V.I., and Yakeron, V.I., *Khim. Prom-st.*, 1996, vol. 95, no. 2, p. 29.
30. Koruabkina, N.A., Ushakov, V.A., and Ismagilov, Z.R., *Second Russian-Korean Joint Seminar on Energy Catalysts*, Novosibirsk, 1997, p. 54; Ismagilov, Z.R. and Kerzhentsev, M.A., *Zh. Vses. Khim. O-va. im. D. I. Mendeleva*, 1990, vol. 35, no. 1, p. 43.
31. Altynbekova, K.A., Popova, N.M., and Sokolova, L.A., *Seminar pamyati professora V.V. Popovskogo "Zakonomernosti glubokogo okisleniya veshchestv na tverdykh katalizatorakh"* ("Deep Oxidations on Solid Catalysts," Professor V.V. Popovskii Memorial Seminar), Novosibirsk, 2000, p. 149.
32. Grigor'eva, V.P., Popova, N.M., Zheksenbaeva, Z.T., Sass, A.S., Salakhova, R.Kh., and Dosumov, K., *Izv. Minist. Obraz. Nauki Resp. Kaz., Nats. Akad. Nauk. Resp. Kaz., Ser. Khim.*, 2002, no. 5, p. 63.
33. Komashko, L.V., Zheksenbaeva, Z.T., Popova, N.M., and Dosumov, K., *Izv. Minist. Obraz. Nauki Resp. Kaz., Nats. Akad. Nauk. Resp. Kaz., Ser. Khim.*, 2002, no. 6, p. 68.
34. Popova, N.M., Kosmambetova, G.R., Sokolova, L.A., Davydov, A.A., Dosumov, K., Demidov, A.V., and Zheksenbaeva, Z.T., *Izv. Minist. Obraz. Nauki Resp. Kaz., Nats. Akad. Nauk. Resp. Kaz., Ser. Khim.*, 2000, no. 6, p. 23.
35. Vorob'ev, V.N., Nivarov, V.A., and Khasanov, K.Kh., *Kinet. Katal.*, 1984, vol. 25, no. 3, p. 712.
36. Rode, A.A., *Pochvennaya vлага* (Soil Moisture), Moscow: Akad. Nauk SSSR, 1952.
37. Popova, N.M., Kosmambetova, G.R., Sokolova, L.A., Dosumov, K., and Zheksenbaeva, Z.T., *Zh. Fiz. Khim.*, 2001, vol. 75, no. 1, p. 44 [Russ. J. Phys. Chem. (Engl. Transl.), vol. 75, no. 1, p. 37].
38. Kirchnerova, G. and Klvana, D., *Catal. Lett.*, 2000, vol. 67, p. 175.
39. Artizzu-Duart, P., Brulle, Y., Garbowski, E., Guilhaume, N., and Primet, M., *Catal. Today*, 1999, vol. 54, p. 181.
40. Artizzu-Duart, P., Millet, J.M., Guilhaume, N., Garbowski, E., and Primet, M., *Catal. Today*, 2000, vol. 59, p. 163.
41. Popova, N.M., Marchenko, E.A., Zheksenbaeva, Z.T., and Dosumov, K., *Tezisy Mezhdunarodnoi konferentsii "Problemy kataliza 21 veka"* (Proc. Int. Conf. on Problems of Catalysis in the 21st Century), Almaty, 2000, p. 94.
42. Chimino, S., Zisi, Z., Pirone, R., Puss, G., and Turco, M., *Catal. Today*, 2000, vol. 59, p. 19.
43. Groppi, G., Cristiani, C., and Forzatti, P., *5th European Congress on Catalysis, Symp. 01: New Catalytic Materials for New or Improved Processes*, Limerick, Ireland, 2001, p. 24.